

Surface-barrier structure of Cu(001) from analysis of low-energy electron diffraction

M. N. Read

*School of Physics, University of New South Wales, P. O. Box 1,
Kensington, New South Wales, Australia 2033*

(Received 22 April 1985)

High-resolution intensity measurements obtained by Dietz, McRae, and Campbell for low-energy electron diffraction from Cu(001) have been analyzed using an exact scattering treatment and a linear saturated image-barrier model. Theoretical fits of maxima and minima to ~ 0.3 eV can be obtained by a range (~ 6 a.u.) of values of z_0 , the origin of the image surface potential. A fit to 0.05 eV is obtained for $z_0 = -3.7$ a.u. from the first row of atoms. Further experimental data at other incident angles must be similarly analyzed before this surface-barrier model can be confirmed for Cu(001).

Beam-intensity data from low-energy electron diffraction (LEED) at crystal surfaces can contain fine-structure features which arise when the backscattered electron has insufficient energy, associated with its component of momentum normal to the surface, to be transmitted by the surface potential barrier and is reflected back to the crystal. The detailed mechanism responsible for the intensity fluctuations is given by McRae.¹⁻³ By assuming different models for the electron surface potential barrier and calculating profiles which fit experimental data, it is hoped that details of the shape and location of the barrier can be found.

Dietz, McRae, and Campbell (DMC) have recently obtained high-resolution intensity data from a Cu(001) surface showing two fully resolved peaks in the Rydberg series near the $\bar{1}\bar{1}$ beam threshold at $\theta = 61.7^\circ$ and (11) azimuth.² They analyzed the data using a one-dimensional barrier model of the form suggested by Appelbaum and Hamann⁴ and Lang and Kohn.⁵ This model was found to be consistent with all the experimental data but its parameters could not be obtained because both barrier and substrate scattering could only be treated approximately.

This paper analyzes the data using the same form of saturated image-barrier model suggested in Ref. 2 and using the full dynamical scattering theory of Kambe-McRae.⁶ In these calculations the elastic scattering potential of the crystal is represented in the muffin-tin form and is the self-consistent crystal band-structure potential of Snow and Waber⁷ with Slater exchange-correlation coefficient $\alpha = 1$. The constant potential between muffin-tin spheres represents the average elastic scattering potential U_{el} of the conduction electrons in the bulk crystal and is taken as the zero of energy. The crystal inelastic scattering potential iU_{in} simulates the loss of electrons from the incident beam due to inelastic collisions associated with the conduction electrons in the bulk region of the crystal. From photoemission data, McRae and Caldwell⁸ have estimated U_{in} for Cu(001) for incident electrons in the energy range 0–10 eV above the vacuum level. Their result is

$$-U_{in}(E) = 0.26(1 + E/\phi)^{1.7}(\text{eV}), \quad (1)$$

where E is the energy of incident electrons with respect to the vacuum level and ϕ the electron work function for Cu(001) = 4.5 eV. Therefore, $U_{in}(E = 10 \text{ eV}) = -1.85 \text{ eV} = -0.136 \text{ Ry}$ and this constant value is used at all energies in the present calculations. The total electron scattering po-

tential of the bulk crystal is then

$$U = U_{el} + iU_{in} = 0 - 0.136i(\text{Ry}) \quad (2)$$

At a perpendicular distance z_j from the center of the first row of atoms in the crystal, the potential U joins onto the electron scattering potential of the surface conduction electrons which is also called the surface-barrier potential U^b . z_j is here chosen to be at the jellium discontinuity. U^b is modeled by the average one-dimensional linear saturated image barrier (SIB) suggested by DMC based on the results in Refs. 4 and 5. The positive z axis is chosen to be perpendicular to the crystal surface and directed into the crystal with the origin at the center of the first row of atoms at the surface. For distances < -5 a.u. from the origin, this model consists of the classical image potential with an origin shift z_0 . Closer to the surface this potential is smoothly joined onto a linear form to represent the weakening and saturation of the image form. The surface-barrier model in Rydberg atomic units is then

$$U^b = U_{el}^b + iU_{in}^b, \quad (3)$$

where

$$U_{el}^b(z) = U_0 + 1/[2(z - z_0)] \quad \text{for } z \leq z_m, \quad (4a)$$

$$= -(z - z_j)/[2(z_m - z_0)^2] + U_s \quad \text{for } z_m < z < z_j, \quad (4b)$$

and z_m is the match point where the image and linear parts of the potential join smoothly, and is given by

$$z_m = z_0 + 1/(2U_s) - [(z_0 - z_j)/2U_0 + 1/U_s^2]^{1/2}. \quad (5)$$

U_s is the value of the surface-barrier potential energy with respect to the crystal zero of potential at the jellium discontinuity z_j , z_0 is the origin of the $1/[2(z - z_0)]$ image form, and U_0 is the height of the potential-energy barrier with respect to the crystal zero. U_0 can be estimated⁹ for very low energy incident electrons from the sum of the Fermi level with respect to the crystal zero for the particular scattering potential used and the electron work function for the particular surface. Hence, a value of $U_0 = 0.88 \text{ Ry}$ (12 eV) was chosen for these calculations.

$$U_{in}^b(z) = -U_{in} \exp[-(z - z_j)^2/\alpha^2], \quad (6)$$

where α is the half-width of the above Gaussian function centered at z_j and McRae and Caldwell¹⁰ have estimated α

to be $\sim 1 \text{ \AA} = 1.85 \text{ a.u.}$ The linear SIB model is drawn to scale in Fig. 1. Also shown is the classical image barrier (IB) with origin shift to z_0 , which is truncated at the inner potential, and a modified image barrier (MIB) which has slight saturation and joins onto the inner potential in a smooth manner. These models are described in more detail in Ref. 11.

Frame 1 of Fig. 2 reproduces the experimental data obtained by DMC.² They report that these data were separately normalized to unity above and below 12 eV. The experimentally resolved maxima occur at 11.25, 12.67, and 12.92 eV with minima at 12.15 and 12.85 eV. Frame 3 shows the best-fit theoretical profile calculated in the present work using the linear SIB model proposed by DMC² and described in Eqs. (3)–(6). An energy interval of 0.02 eV was used in the computations for energies above 11.2 eV. A Rydberg series of fine structure is seen to be associated with the emergence of both the $(0\bar{1}, \bar{1}0)$ and $\bar{1}\bar{1}$ beams. In frame 2, the theoretical profile is convoluted with a Gaussian function of half-width $\sigma = 0.03 \text{ eV}$ to simulate experimental effects of spatial and energy spread in the incident electron beam. Comparison of this convoluted profile with the experimental data shows a fit of all major maxima and minima positions to within 0.05 eV.

The SIB model has three parameters: U_0 , z_0 , and U_s . The intensity fine-structure features closer to beam thresholds depend more on the form of the barrier at large distances from the surface and hence the parameter z_0 , whereas features far from thresholds depend on the barrier form closer to the metal substrate.^{2,3} It would not be expected that the one-dimensional truncated image (IB) and MIB models would be adequate to describe fine-structure features far from beam thresholds. Similarly, the average one-dimensional linear SIB model used here, with the discontinuous drop at z_j , would not be adequate to describe

features far from beam thresholds, but it is hoped it may be sufficiently accurate to describe features $\sim 3 \text{ eV}$ from threshold for large incident angles. This would enable the origin of the image potential z_0 for a particular surface to be determined.

In general, moving the origin of the image tail z_0 farther from the metal substrate results in movement of the interference fringes in the intensity profile to lower energies; increasing the value of U_s moves the fringes to higher energies. By corresponding adjustment of z_0 and U_s it is possible to produce an intensity maximum at one particular energy position for a continuous range ($\sim 6 \text{ a.u.}$) of corresponding values of z_0 and U_s . The method used to fit the experimental data proceeded as follows. As the lowest energy peak shows greatest sensitivity to barrier model and parameters the full set of corresponding U_s and z_0 which produce a maximum at 11.25 eV for $U_0 = 12 \text{ eV}$ were found.¹² For a wide range of this set of parameters, the higher energy minima and maxima were also fitted to at least $\sim 0.3 \text{ eV}$. Therefore, it is not possible to determine the origin of the image tail z_0 from a match of data of this type to only $\sim 0.3 \text{ eV}$. The unique set of $U_s = 0.48 \text{ Ry}$ (5.4 eV) and $z_0 = -3.7 \text{ a.u.}$ (-2.0 \AA) for $U_0 = 12 \text{ eV}$ was then obtained from the best fit of the higher energy maxima and minima. That is, the correct parameters were only obtainable from a match of the minimum at 12.15 eV and the maximum at 12.67 eV (as well as the overall shape of the profile).

The pronounced effect of the strong saturation of the SIB model can be seen from the profile in frame 4 of Fig. 2 where the MIB model is used with the same z_0 and U_0 parameters. The effect on the profile of the difference between the two models is that the lower energy minima and maxima are substantially altered but the higher energy features associated with the image part of the potential are not.

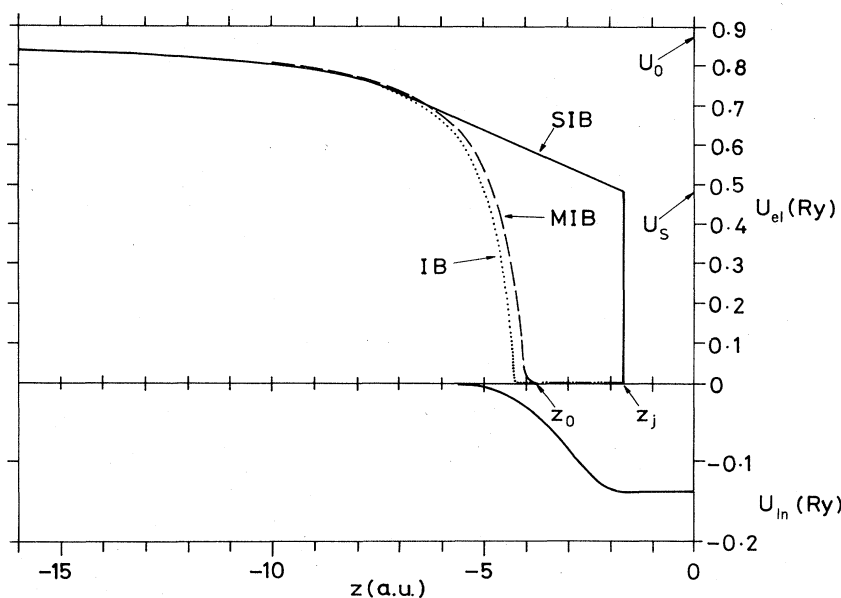


FIG. 1. Plots to scale of models of the electron potential energy U near a metal surface. U_{el} and iU_{in} are the elastic and inelastic scattering potentials, respectively. The full line in the upper frame is for the linear saturated-image-barrier (SIB) model. The dotted line shows the truncated classical image barrier (IB) with origin shift to z_0 . The dashed line shows the modified image barrier (MIB) of Ref. 11. The parameters for each model are the same as those used in the calculations shown in Fig. 2. $1 \text{ Ry} = 13.6 \text{ eV}$ and $1 \text{ a.u.} = 0.529 \text{ \AA}$.

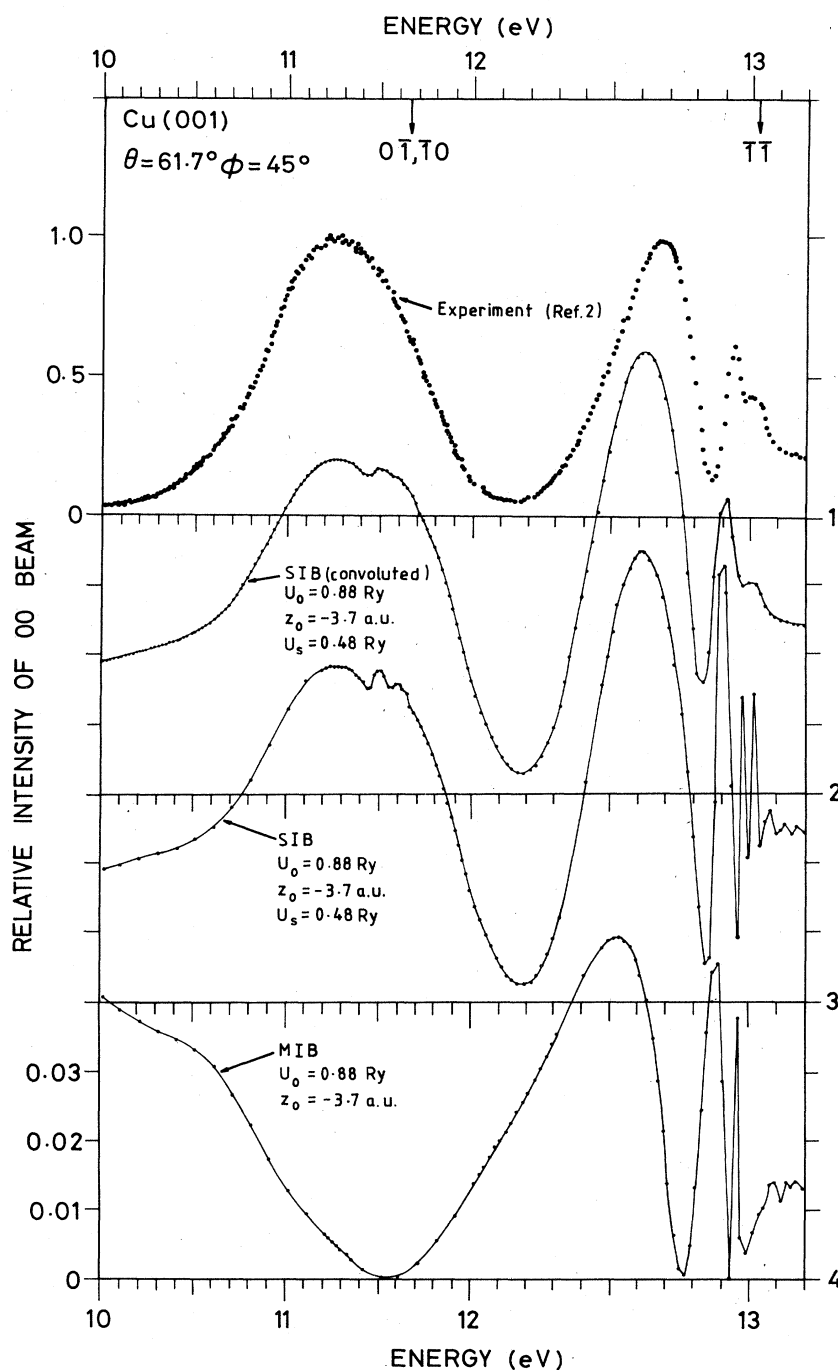


FIG. 2. Relative intensity of the 00 beam with respect to intensity of the incident beam for the Cu(001) surface at $\theta=61.7^\circ$, $\phi=45^\circ$. The energies of emergence of the $(0\bar{1}, 10)$ and 11 beams are marked by downward arrows. Frame 1 shows the experimental data of Dietz, McRae, and Campbell from Ref. 2. Frame 2 shows the calculated profile using the linear SIB model with best-fit parameters as shown and convoluted with a Gaussian function (see text). Frame 3 shows the profile in frame 2 before convolution. Frame 4 shows the calculated profile for the MIB model with parameters as shown. Note that the scale is expanded for energies > 12 eV.

The theoretical analysis by DMC² used the linear SIB model but was only approximate because the crystal substrate scattering properties were incorporated as an adjustable parameter with no variation with energy and scattering between crystal substrate and surface-barrier potentials were also treated approximately. This resulted in a set of

approximate best-fit parameters which produced a fit of the data to < 0.05 eV. With the present exact analysis only one set of parameters should achieve this fit. These are $z_0 = -2.0$ a.u. (-1.1 Å) from the jellium discontinuity $z_j = -1.7$ a.u. and potential depth at z_j with respect to the vacuum level of $U_D = 0.40$ Ry (5.4 eV) and they differ in

U_D by only $\sim 14\%$ with one set, $z_0 = -2.0$ a.u. and $U_D = 4.7$ eV, on the line of best-fit parameters obtained by DMC.

Jennings, Thurgate, and Price¹³ have also analyzed this experimental data and their own using the SIB model and concluded that for Cu(001) the origin of the image potential is $z_0 = -2.5 \pm \sim 0.5$ a.u. from the first row of atoms and $U_s = 4.1$ eV or $U_D = 6.8$ eV. However, their experimental and theoretical maxima fitted to 0.05 eV but the minima to only 0.3 eV. Their previous determination of z_0 for Cu(001) was $z_0 = -1.3 \pm 0.3$ a.u. (Ref. 14) and then $z_0 = -1.6 \pm 0.1$ a.u. (Ref. 15) from a match of data with this order of discrepancy. The parameters determined by them are also less consistent with the line of best-fit parameters found by DMC and the present fit for $z_0 = -3.7$ a.u. and $U_s = 5.4$ eV is not included in their range.

Gaubert *et al.*¹⁶ have recently analyzed in detail the threshold effects in the present intensity profile and concluded that the major origin of the saturated (discontinuous) barrier profile must be attributed to the theoretical simplifications used by DMC in addition to some confusion concerning the normalization of the experimental data. The present result suggests that this conclusion is not correct since the use of an exact scattering analysis for the model barrier and substrate potentials produces very good agreement with experiment and the best-fit parameters are only slightly different from a set on DMC's line of best-fit parameters.

Recently the same experimental data was again analyzed

using the MIB and an exact scattering treatment. That work⁹ concluded that the MIB model with $z_0 = -5.2 \pm \sim 0.2$ a.u. and $z_0 = -8.6 \pm \sim 0.3$ a.u. also provides a fit to all features of the present experimental data to within 0.05 eV.

The main conclusions are that both the linear SIB with $z_0 = -3.7$ a.u. and $U_s = 5.4$ eV and the MIB, with negligible saturation and with the previously noted parameters, both provide a fit of the experimental data to within 0.05 eV. The best model for the surface barrier ~ 5 a.u. from the center of the first row of atoms on Cu(001) and the origin of the image tail z_0 cannot be deduced until further experimental data at other incident angles are analyzed. It is possible that a slight adjustment of the present best-fit parameters of the SIB model will provide an even better fit to the data. This analysis and an estimate of the uncertainty limits on the parameters z_0 and U_s , due to their dependence on U_0 ,⁹ are in progress.¹²

For sets of intensity data obtained at large incident angles showing a number of fine-structure features which arise from surface-barrier scattering and which are ~ 3 eV from beam thresholds, it is not possible to attempt to deduce the origin of the image potential unless fits of theoretical and experimental maxima and minima to at least 0.05 eV are obtained. For this type of data and the three-parameter SIB model, fits of the order of 0.3 eV can be achieved for a continuous range of values of z_0 from ~ 1 –7 a.u. by corresponding adjustment of the parameter U_s .

¹E. G. McRae, Rev. Mod. Phys. **51**, 541 (1979).

²R. E. Dietz, E. G. McRae, and R. L. Campbell, Phys. Rev. Lett. **45**, 1139 (1980).

³E. G. McRae, D. T. Pierce, G.-C. Wang, and R. J. Celotta, Phys. Rev. B **24**, 4230 (1981); D. T. Pierce, R. J. Celotta, G.-C. Wang, and E. G. McRae, Solid State Commun. **39**, 1053 (1981).

⁴J. A. Appelbaum and D. R. Hamann, Phys. Rev. B **6**, 1122 (1972).

⁵N. D. Lang and W. Kohn, Phys. Rev. B **7**, 3541 (1973).

⁶K. Kambe, Z. Naturforsch. Teil A **22**, 322 (1967); **23**, 1280 (1968); E. G. McRae, Surf. Sci. **11**, 479 (1968); **25**, 491 (1971).

⁷E. C. Snow and J. T. Waber, Phys. Rev. **157**, 570 (1967).

⁸E. G. McRae and C. W. Caldwell, Surf. Sci. **57**, 766 (1976).

⁹M. N. Read, Appl. Surf. Sci. (to be published).

¹⁰E. G. McRae and C. W. Caldwell, Surf. Sci. **57**, 77 (1976).

¹¹M. N. Read and P. J. Jennings, Surf. Sci. **74**, 54 (1978).

¹²M. N. Read (unpublished).

¹³P. J. Jennings, S. M. Thurgate, and G. L. Price, Appl. Surf. Sci. **13**, 180 (1982).

¹⁴G. L. Price, P. J. Jennings, P. E. Best, and J. C. L. Cornish, Surf. Sci. **89**, 151 (1979).

¹⁵P. J. Jennings and G. L. Price, Surf. Sci. **93**, L124 (1980).

¹⁶G. Gaubert, R. Baudoing, Y. Gauthier, J. C. Le Bosse, and J. Lopez, J. Phys. C **16**, 2625 (1983).